Solitons in the periodic Korteweg–de Vries equation, the Θ-function representation, and the analysis of nonlinear, stochastic wave trains

A. R. Osborne
Istituto di Fisica Generale dell'Università, Via Pietro Giuria 1, Torino 10125, Italy
(Received 20 June 1994; revised manuscript received 19 January 1995)

The Korteweg–de Vries (KdV) equation and its single, periodic cnoidal wave solution have been known for a century. The present paper focuses on *N-degree of freedom cnoidal wave solutions to the KdV equation* (here N ranges up to 1000) and addresses some of the issues necessary for the practical implementation of the formalism in both theoretical and experimental physics. To this end, the Θ-function representation is exploited and it is shown that an important class of solutions to the periodic KdV equation consists of a linear superposition of N cnoidal waves plus their mutual nonlinear interactions. The formulation may be viewed as a generalization of ordinary, periodic Fourier series to nonlinear, integrable wave motion. Each cnoidal wave is a nonlinear spectral component in the theory and has a form that depends upon the value of its modulus m, $0 \le m \le 1$. The waves generally take the familiar shape of sine waves ($m \sim 0$), Stokes waves ($m \sim 0.5$), and solitons ($m \sim 1$). A number of applications and aspects of the Θ-function approach are addressed, including (1) solutions of the periodic KdV equation for which statistical mechanical and stochastic realizations may be analyzed in terms of random soliton modes interacting with a random radiation sea, (2) the numerical computation of N-degree-of-freedom solutions to the periodic KdV equation, (3) the time series analysis of experimental shallow water wave data, (4) the fractal structure of the wave numbers and phases in KdV wave trains. The results of these studies are seen to improve the physical understanding of nonlinear wave dynamics governed by the periodic KdV equation.

PACS number(s): 03.40.Gc

I. INTRODUCTION

The inverse scattering transform generally solves certain nonlinear partial differential equations that have soliton solutions. The Cauchy problem for these equations, with both infinite-line and periodic boundary conditions, has been studied extensively [1–21]. In the present paper I focus on solutions to soliton equations that have periodic boundary conditions such that stationarity and ergodicity are ensured [22]. The physical reason for considering this class of wave trains is to allow application of the results to nonlinear wave dynamics in the laboratory [23,24], to ocean surface waves [25,26], to nonlinear statistical mechanics, and to stochastic dynamics [22,27]. In these studies the focus has been on the Korteweg–de Vries (KdV) equation, which generally describes the propagation of nonlinear long waves in dispersive media [1–5,28].

The above physical problems have previously been studied extensively in the so-called hyperelliptic function representation [29–35], in which periodic solutions to the KdV equation are computed as the linear superposition of a set of nonlinear waves referred to as hyperelliptic-function oscillation modes. In the present paper periodic motions of the KdV equation are studied in an alternative basis called the Θ-function representation. This latter formulation, which arises as an algebraic geometric linearization of the hyperelliptic modes [10–14], is exploited here as a tool for studying a number of interesting problems in nonlinear wave physics.

To this end the applications of the Θ-function formulation discussed below have been made possible by a number of recent advances in numerical analysis [29–36], which substantially speed up the requisite computer calculations. The present paper develops several results that shed light on certain physical aspects of periodic, nonlinear wave motions known to be integrable by the inverse scattering transform. Why, when hyperelliptic functions have been shown to be so useful in previous work [22–27], do I now consider the Θ-function representation? What advantages, if any, do Θ functions have over hyperelliptic functions for the study of nonlinear wave dynamics? A major objective of this paper is to suggest that Θ functions, long neglected because they are so difficult to compute numerically, may instead, thanks to improvements in numerical algorithms, offer an alternative approach that compliments previous studies using hyperelliptic functions. A major goal for this paper is to document some of these results.

In order to address the physical perspective given herein it has been necessary to develop a number of mathematical results with regard to the Θ functions. These results are provided in Theorems 1–3 given in the sections below, where interpretations in terms of nonlinear wave physics are also provided. In order to set the stage for what follows I first address the periodic, traveling-wave solution to the KdV equation, the cnoidal wave.

A. Cnoidal wave solution of the KdV equation

The KdV equation is given by

$$\eta_t + c_0\eta_x + \alpha\eta\eta_x + \beta\eta_{xxx} = 0 , \quad 0 \le x \le L \tag{1.1}$$

for L the spatial period. The coefficients c_0, α, and β depend on the particular physical application. For surface water waves $c_0=\sqrt{gh}$, $\alpha=3c_0/2h$, and $\beta=c_0h^2/6$, where h is the water depth and g is the acceleration of gravity. The important parameter $\lambda=\alpha/6\beta$, a ratio of nonlinearity to dispersion, is used below in the inverse scattering transform formulation. Many physical applications of the KdV equation are known and are discussed in the literature [1–7,28].

Korteweg and deVries [37], 100 years ago, found their equation (1.1) and an associated periodic traveling-wave solution that is known as the *cnoidal wave:*

$$\eta(x,t)=\frac{4k^2}{\lambda}\sum_{n=1}^{\infty}\frac{n(-1)^nq^n}{1-q^{2n}}\cos[nk(x-c_0t)]$$
$$=2A_0\mathrm{cn}^2([K(m)/\pi][k(x-C_0t)];m)\ . \quad (1.2)$$

The Jacobian elliptic function cn has modulus m given by

$$mK^2(m)=\frac{3\pi^2A_0}{2k^2h^3}=4\pi^2U\ ,\quad U=\frac{3A_0}{8k^2h^3}\ . \quad (1.3)$$

A_0 is the amplitude of the cnoidal wave, U is the Ursell number, k is the wave number, and h is the water depth. $K(m)$ is the usual elliptic integral [38,39]. The nonlinear phase speed C_0 of the cnoidal wave has the formula

$$C_0=c_0\{1+2A_0/h-2k^2h^2K^2(m)/3\pi^2\}\ . \quad (1.4)$$

The series representation given in (1.2) for the cnoidal wave is the Stokes series solution to the KdV equation [8]. When the modulus $m\to 0$ the cnoidal wave reduces to a sine wave; when $m\to 1$ the cnoidal wave approaches a solitary wave or soliton. The KdV equation thus offers a way to simultaneously include both nonlinearity (the term $\alpha\eta\eta_x$) and dispersion ($\beta\eta_{xxx}$) in a simple model (1.1). In fact, it is the balance between nonlinearity and dispersion that gives rise to the stability of the soliton solutions.

B. Fourier analysis of the linearized KdV equation

The periodic traveling-wave solution to the linearized KdV equation with periodic boundary conditions [set $\alpha=0$ in (1.1)]

$$\eta_t+c_0\eta_x+\beta\eta_{xxx}=0,\quad 0\le x\le L \quad (1.5)$$

is a simple cosine function $a\cos(kx-\omega t+\phi)$, where $k=2\pi/L$ is the wave number, L is the spatial period, a is the wave amplitude, and ϕ is the phase. Here k and ω are the usual wave number and frequency, linked by the dispersion relation $\omega=\omega(k)$ [see (1.8) below]. Spectral solutions to the linearized KdV equation (1.5) can be written as a linear superposition of these simple solutions, i.e., as an ordinary Fourier series for N degrees of freedom,

$$\eta(x,t)=\sum_{j=1}^{N}a_j\cos(k_jx-\omega_jt+\phi_j) \quad (1.6)$$

[see Ref. [30] for a discussion of the linear problem (1.6) written in terms of inverse scattering transform variables]. Here the a_j are the Fourier coefficients and the ϕ_j are the Fourier phases. The commensurable wave numbers k_j are given by

$$k_j=2\pi j/L \quad (1.7)$$

and the associated incommensurable frequencies ω_j are governed by the dispersion relation of (1.5),

$$\omega_j=c_0k_j-\beta k_j^3\ . \quad (1.8)$$

One is often interested in the Cauchy problem for the linearized KdV equation, where $\eta(x,t=0)$ is assumed to be known and $\eta(x,t)$, for all t, is then sought. To this end the Fourier transform of a wave train $\eta(x,0)$ consists of the set of Fourier amplitudes and phases $\{a_j,\phi_j\}$ for $1\le j\le N$. Time evolution of the wave motion $\eta(x,t)$ then arises by inclusion of the ω_jt term in the cosine of (1.6).

The fact that periodic Fourier series solutions (1.6) to the linearized KdV equation (1.5) can be easily represented spectrally as a linear superposition of N sine waves raises a fundamental question: Can the solutions to periodic KdV (1.1) be represented in terms of N cnoidal waves (1.2) using a nonlinear generalization of Fourier analysis? Section II addresses this issue from a concrete point of view and provides a simple analytical and numerical scenario for its resolution, i.e., it is shown that periodic solutions to KdV can be represented as a linear superposition of cnoidal waves plus their mutual nonlinear interactions. In order to give perspective on these results, a comparison is given in Sec. III between the infinite-line Hirota N-soliton solution to the KdV equation and the Θ-function solutions of the associated periodic problem. In Sec. IV motivation is given for a Fourier interpretation of the Θ functions and how they can be exploited in terms of power spectral analysis. A rather interesting result, also discussed in this section, is how the wave numbers, while commensurable in the ordinary Fourier sense, are statistically distributed on a fractal set. This result has important implications on the numerical computation of Θ functions, i.e., why they are so difficult to compute. Finally, in Sec. V a number of physical applications of Θ functions are considered, including the numerical computation of N-degree-of-freedom solutions of the KdV equation, stochastic solutions of the equation, and the analysis of ocean surface wave data. The conclusions are provided in Sec. VI.

II. Θ-FUNCTION SOLUTIONS OF THE KdV EQUATION

While (1.6) solves the linearized KdV equation (1.5) for periodic boundary conditions, the periodic KdV equation itself (1.1) is nonlinear and hence requires considerable analysis to obtain the analogous nonlinear generalization of Fourier series [10–12]. The KdV equation has rather general periodic solutions that may be written in terms of the Θ-function representation of the inverse scattering transform

$$\lambda\eta(x,t)=2\frac{\partial^2}{\partial x^2}\ln\Theta_N(\eta_1,\eta_2,\ldots,\eta_N)\ , \quad (2.1)$$

where the N-dimensional Θ-function Θ_N is given by

$$\Theta_N(\eta_1,\eta_2,\ldots,\eta_N)=\sum_{M_1=-\infty}^{\infty}\sum_{M_2=-\infty}^{\infty}\cdots\sum_{M_N=-\infty}^{\infty}\exp\left[i\sum_{j=1}^{N}M_j\eta_j+\tfrac{1}{2}\sum_{i=1}^{N}\sum_{j=1}^{N}M_iB_{ij}M_j\right]. \tag{2.2}$$

A spectral solution (2.1) and (2.2) of the KdV equation has N degrees of freedom and Θ-function phases given by

$$\eta_j=k_jx-\omega_jt+\phi_j\ ,\quad 1\le j\le N\ . \tag{2.3}$$

Here the k_j are the wave numbers, the ω_j are the frequencies, and the ϕ_j are the phases. The interaction (or period) matrix $\underline{B}=\{B_{ij}\}$ contains the amplitudes of the N degrees of freedom on the diagonal terms; the off-diagonal terms determine the nonlinear interactions among the degrees of freedom. The parameters in this formulation k_j, ω_j, ϕ_j, and B_{ij} are computable from the Floquet spectrum of the associated Schrödinger eigenvalue problem (the spectral equation for the KdV equation) and from the Jacobian transformation of algebraic geometry, which linearizes the hyperelliptic function representation of the flow [10–16]; analytical and numerical determination of these parameters are discussed in detail elsewhere (see [36] and references cited therein) and briefly in the Appendix.

A major focus in the present paper is to address the following inquiry: Are the Θ functions (2.2) physically useful for the study of nonlinear wave motions? While the answer is in the affirmative, the actual analytical and numerical exploitation of the approach has not been easy [10–21,40,41]. A number of directions are motivated here for applying Θ functions to physical problems as discussed in detail below. As a consequence, a major effort to better understand certain properties of Θ functions has also been made.

To this end, in what follows, the notation in (2.1)–(2.3) is changed to vector form, i.e., the Θ phases are written

$$\boldsymbol{\eta}=\mathbf{k}x-\boldsymbol{\omega}t+\boldsymbol{\phi}=(\eta_1,\eta_2,\ldots,\eta_N)\ , \tag{2.4}$$

where the wave numbers, the frequencies, and the constant phases are given by

$$\begin{aligned}&\mathbf{k}=(k_1,k_2,\ldots,k_N)\ ,\\ &\boldsymbol{\omega}=(\omega_1,\omega_2,\ldots,\omega_N)\ ,\\ &\boldsymbol{\phi}=(\phi_1,\phi_2,\ldots,\phi_N)\ .\end{aligned} \tag{2.5}$$

Note further that

$$\begin{aligned}&\mathbf{M}\cdot\boldsymbol{\eta}=(\mathbf{M}\cdot\mathbf{k})x-(\mathbf{M}\cdot\boldsymbol{\omega})t+\mathbf{M}\cdot\boldsymbol{\phi}\ ,\\ &\mathbf{M}=(M_1,M_2,\ldots,M_N)\ .\end{aligned} \tag{2.6}$$

The integer entries $(M_1,M_2,\ldots,M_N)$ in the vector $\mathbf{M}$ are the summation indices in Eq. (2.2). It is then convenient to write (2.2) in the vector form

$$\Theta_N(\boldsymbol{\eta})=\sum_{\mathbf{M}}e^{i\mathbf{M}\cdot\boldsymbol{\eta}+(1/2)\mathbf{M}^T\cdot\underline{B}\cdot\mathbf{M}}\ , \tag{2.7}$$

where the superscript T denotes transposition.

A cautionary note is worth making with regard to the notation used herein. In particular the symbol M has been used in a number of contexts in the present paper. Note that the simple scalar M indicates the truncation limit in the Θ-function summation as discussed with regard to Theorem 3 below. Values of the variable M with a subscript, M_j, are the components of the vector $\mathbf{M}$, which is bold; this has been defined in (2.6) and will be exploited in Theorems 1 and 2 below.

In the notation of (2.7) it is straightforward to address the following theorem.

Theorem 1: Cnoidal Wave Theorem. The Θ-function solution to the KdV equation (2.1), (2.2) can be written in the following form $[u(x,t)\equiv\lambda\eta(x,t)]$:

$$u(x,t)=2\frac{\partial^2}{\partial x^2}\ln\Theta_N(\boldsymbol{\eta})=u_{\rm cn}(\boldsymbol{\eta})+u_{\rm int}(\boldsymbol{\eta}) \tag{2.8}$$

The subscript "cn" on the right-hand side of the equation refers to contributions to the solution that are a linear superposition of cnoidal waves. The subscript "int" on the right-hand side of Eq. (2.8) refers to nonlinear interactions among the cnoidal waves. These terms have the following specific forms:

$$\begin{aligned}&u_{\rm cn}(\boldsymbol{\eta})=2\frac{\partial^2}{\partial x^2}\ln G(\boldsymbol{\eta})\ ,\\ &u_{\rm int}(\boldsymbol{\eta})=2\frac{\partial^2}{\partial x^2}\ln\left\{1+\frac{F(\boldsymbol{\eta},C)}{G(\boldsymbol{\eta})}\right\}\end{aligned} \tag{2.9}$$

and

$$\begin{aligned}&F(\boldsymbol{\eta},C)=\sum_{\mathbf{M}}Ce^{i\mathbf{M}\cdot\boldsymbol{\eta}+(1/2)\mathbf{M}^T\cdot\underline{D}\cdot\mathbf{M}}\ ,\\ &C=[e^{(1/2)\mathbf{M}^T\cdot\underline{Q}\cdot\mathbf{M}}-1]\ ,\\ &G(\boldsymbol{\eta})=F(\boldsymbol{\eta},1)\end{aligned} \tag{2.10}$$

The interaction matrix $\underline{B}=\underline{D}+\underline{Q}$ has diagonal $\underline{D}$ and off-diagonal $\underline{Q}$ parts.

Proof. Theorem 1 follows naturally from Eqs. (2.1) and (2.2). Use $\underline{B}=\underline{D}+\underline{Q}$ in (2.7) and write

$$\Theta_N(\boldsymbol{\eta})=\sum_{\mathbf{M}}e^{i\mathbf{M}\cdot\boldsymbol{\eta}+(1/2)\mathbf{M}^T\cdot\underline{D}\cdot\mathbf{M}}+\left\{\sum_{\mathbf{M}}e^{i\mathbf{M}\cdot\boldsymbol{\eta}+(1/2)\mathbf{M}^T\cdot\underline{B}\cdot\mathbf{M}}-\sum_{\mathbf{M}}e^{i\mathbf{M}\cdot\boldsymbol{\eta}+(1/2)\mathbf{M}^T\cdot\underline{D}\cdot\mathbf{M}}\right\},$$

$$\Theta_N(\boldsymbol{\eta})=\sum_{\mathbf{M}}e^{i\mathbf{M}\cdot\boldsymbol{\eta}+(1/2)\mathbf{M}^T\cdot\underline{D}\cdot\mathbf{M}}+\left\{\sum_{\mathbf{M}}[e^{(1/2)\mathbf{M}^T\cdot\underline{Q}\cdot M}-1]e^{i\mathbf{M}\cdot\boldsymbol{\eta}+(1/2)\mathbf{M}^T\cdot\underline{D}\cdot\mathbf{M}}\right\},$$

$$\Theta_N(\boldsymbol{\eta})=\sum_{\mathbf{M}}e^{i\mathbf{M}\cdot\boldsymbol{\eta}+(1/2)\mathbf{M}^T\cdot\underline{D}\cdot\mathbf{M}}\left\{1+\frac{\sum_{\mathbf{M}}[e^{(1/2)\mathbf{M}^T\cdot\underline{Q}\cdot\mathbf{M}}-1]e^{i\mathbf{M}\cdot\boldsymbol{\eta}+(1/2)\mathbf{M}^T\cdot\underline{D}\cdot\mathbf{M}}}{\sum_{\mathbf{M}}e^{i\mathbf{M}\cdot\boldsymbol{\eta}+(1/2)\mathbf{M}^T\cdot\underline{D}\cdot\mathbf{M}}}\right\}.$$

It therefore follows that the solution to the KdV equation can then be written

$$u(x,t)=2\frac{\partial^2}{\partial x^2}\ln\sum_{\mathbf{M}} e^{i\mathbf{M}\cdot\boldsymbol{\eta}+(1/2)\mathbf{M}^T\cdot\underline{D}\cdot\mathbf{M}}+u_{\text{int}}(\boldsymbol{\eta})\ , \tag{2.11}$$

where

$$u_{\text{int}}(x,t)=2\frac{\partial^2}{\partial x^2}\ln\left\{1+\frac{\sum_{\mathbf{M}}[e^{(1/2)\mathbf{M}^T\cdot\underline{Q}\cdot\mathbf{M}}-1]e^{i\mathbf{M}\cdot\boldsymbol{\eta}+(1/2)\mathbf{M}^T\cdot\underline{D}\cdot\mathbf{M}}}{\sum_{\mathbf{M}} e^{i\mathbf{M}\cdot\boldsymbol{\eta}+(1/2)\mathbf{M}^T\cdot\underline{D}\cdot\mathbf{M}}}\right\}\ . \tag{2.12}$$

Simple definitions then lead to the form given in Theorem 1.

To render the cnoidal wave interpretation of the first term on the right-hand side of (2.8) or (2.11) note that the function $G(\boldsymbol{\eta})$ has the product form

$$G(\boldsymbol{\eta})=\sum_{\mathbf{M}} e^{i\mathbf{M}\cdot\boldsymbol{\eta}+(1/2)\mathbf{M}^T\cdot\underline{D}\cdot\mathbf{M}}=\prod_{n=1}^{N} G_n(M_n\eta_n) \tag{2.13}$$

such that G_n is the classical function known as Θ_3 [38,39], which has the following series representation:

$$G_n(\eta_n)=\sum_{M_n=-\infty}^{\infty} e^{iM_n\eta_n+(1/2)M_n^2D_{mn}}\ . \tag{2.14}$$

To prove (2.13) and (2.14) rewrite (2.2) in the form

$$\begin{aligned}\Theta_N(\eta_1,\eta_2,\ldots,\eta_N)=&\sum_{M_1=-\infty}^{\infty}\exp[iM_1\eta_1+\tfrac{1}{2}M_1^2B_{11}]\\ &\times\sum_{M_2=-\infty}^{\infty}\exp[iM_2\eta_2+\tfrac{1}{2}M_2^2B_{22}]\\ &\times\cdots\sum_{M_N=-\infty}^{\infty}\exp[iM_N\eta_N+\tfrac{1}{2}M_N^2B_{NN}]\exp\left[\tfrac{1}{2}\sum_{j=1}^{N}\sum_{\substack{k=1\\k\neq j}}^{N}M_jB_{jk}M_k\right]\ .\end{aligned}$$

Note that in this form the right-hand exponential is over the off-diagonal terms of the period matrix. Then, when the period matrix is taken to be diagonal, as in the present case, the right-hand exponential is just 1 and the above expression reduces to (2.13) and (2.14).

The logarithm of (2.14), setting $m=M_n$, is given by

$$\begin{aligned}&\ln G_n(\eta_n)=\ln\gamma-2\sum_{m=1}^{\infty}\frac{q_n^m}{1-q_n^{2m}}\frac{\cos(m\eta_n)}{m}\ ,\\ &q_n=e^{(1/2)D_{nn}}\ ,\end{aligned} \tag{2.15}$$

where $\eta_n=k_nx-\omega_nt+\phi_n$ and it then follows that

$$\begin{aligned}u_n(x,t)&=2\frac{\partial^2}{\partial x^2}\ln G_n(x,q_n)\\ &=2u_n\mathrm{cn}^2([K(m_n)/\pi][k_n(x-C_nt)+\phi_n];m_n)\ .\end{aligned} \tag{2.16}$$

This is the cnoidal wave (Jacobian elliptic function) solution (1.2) of the KdV equation (1.1); the wave has amplitude u_n. The moduli m_n and phase speeds C_n are given by

$$\begin{aligned}&m_nK^2(m_n)=\frac{3\pi^2A_n}{2k_n^2h^3}=4\pi^2U_n\ ,\\ &C_n=c_0\{1+2A_n/h-2k_n^2h^2K^2(m_n)/3\pi^2\}\end{aligned} \tag{2.17}$$

for $A_n=u_n/\lambda$. Here $K(m)$ is the elliptic integral [38,39] and $U_n=3A_n/8k_n^2h^3$ is the Ursell number [24]. Consequently, from (2.8), (2.10), and (2.11), one finds

$$\begin{aligned}\eta_{\text{cn}}(x,t)&=\frac{u_{\text{cn}}(x,t)}{\lambda}\\ &=2\sum_{n=1}^{N}A_n\mathrm{cn}^2([K(m_n)/\pi][k_n(x-C_nt)+\phi_n];m_n)\ .\end{aligned} \tag{2.18}$$

Note that (2.18) is *not* a solution to the KdV equation since nonlinear interactions have been excluded. Only by adding the nonlinear interaction term (2.12) to (2.18) do we obtain an exact solution to the KdV equation as given by (2.8), or (2.11) and (2.12). Generally speaking, the interaction term u_{int} cannot generally be thought of as a small perturbation to the cnoidal waves u_{cn}, particularly

when the spectrum contains solitons [36]. On the other hand, when the off-diagonal terms $\underline{Q}$ are small

$$e^{(1/2)\mathbf{M}^T\cdot\underline{Q}\cdot\mathbf{M}}-1\sim\tfrac{1}{2}\mathbf{M}^T\cdot\underline{Q}\cdot\mathbf{M}\ .$$

Then one can think of Theorem 1 as representing the relatively weak interactions among N small-amplitude cnoidal waves. This completes the discussion of Theorem 1.

For applications of the periodic inverse scattering transform to the analysis of theoretical and experimental problems it is often convenient to give an interpretation of the formalism in terms of a nonlinear spectrum in the Θ-function representation. This approach differs from the more familiar nonlinear spectral interpretation in terms of the hyperelliptic function representation, which has been documented in detail elsewhere (see Refs. [29–35] and references cited therein). The nonlinear Fourier spectrum in the Θ-function representation consists of the amplitudes of the cnoidal waves at each wave number k_n; the spectral amplitudes $a_n\sim 4q_nk_n^2$ are related to the diagonal terms in the interaction matrix $\underline{B}$ through $q_n=\exp[B_{nn}/2]$ [see (2.12) and (2.13)]. As stated above, the off-diagonal terms $\underline{Q}$ in the $\underline{B}$ matrix determine the nonlinear interactions among the cnoidal-wave spectral components. Thus the B_{ij} term ($i\neq j$) determines the interaction between the ith and the jth cnoidal waves in the spectrum.

Before continuing with the discussion of the theoretical results on the periodic solution to the KdV equation, it is useful to contrast Theorem 1 with the analogous theoretical formulation on the infinite line $-\infty<x<\infty$, i.e., the Hirota N-soliton solution.

III. COMPARISON OF THE PERIODIC Θ-FUNCTION FORMULATION WITH THE HIROTA N-SOLITON SOLUTION

The N-soliton solution to the KdV equation on the infinite x axis ($-\infty<x<\infty$) is given by (see [1] and references cited therein).

$$\lambda\eta(x,t)=2\frac{\partial^2}{\partial x^2}\ln F_N(\eta_1,\eta_2,\ldots,\eta_N)\ ,\quad -\infty<x<\infty\ , \tag{3.1}$$

where

$$F_N(\eta_1,\eta_2,\ldots,\eta_N)=\sum_{\nu_1=0}^{1}\sum_{\nu_2=0}^{1}\cdots\sum_{\nu_N=0}^{1}\exp\left[\sum_{j=1}^{N}\nu_j\eta_j+\tfrac{1}{2}\sum_{i=1}^{N}\sum_{j=1}^{N}\nu_iA_{ij}\nu_j\right]\ . \tag{3.2}$$

The N phases are written

$$\eta_j=k_jx-k_j^3t+\phi_j\ ,\quad 1\le j\le N \tag{3.3}$$

and the $\underline{A}$ matrix has the simple form

$$A_{ij}=\ln\left[\frac{k_i-k_j}{k_i+k_j}\right]^2\ . \tag{3.4}$$

Here the k_i are the soliton wave numbers that are related to the individual soliton amplitudes η_{oi} by $\eta_{oi}=2k_i^2/\lambda$. The N-soliton solution (3.1)–(3.4) has many obvious similarities with the N-cnoidal wave periodic solution (2.1)–(2.3) to the KdV equation, as can be seen by inspection. A number of fundamental differences in the two formulations are, however, immediately obvious. First, in the Hirota formulation the summation of the exponential functions is over the interval $0\le\nu_j\le 1$, while in the Θ function the sum is over $-\infty\le M_j\le\infty$. Second, the single sum over the phases η_j in the argument of the exponential of the Hirota formulation (3.2) is real; in the Θ function (2.2) it is imaginary. Third, it is clear that the parameters in the Hirota formulas, k_j, ϕ_j, A_{ij}, are *not* the same as in the Θ-function representation (see the appendix for a discussion of the parameters in the periodic problem). It is not hard to show that the N-soliton limit of the Θ-function formulation (2.1)–(2.3) is given by the Hirota formulas (3.1)–(3.4); this is accomplished by introducing a Poisson sum formula (see Refs. [17–21] for a detailed discussion of the case for $N=2$).

In Sec. II the solutions to the KdV equation were separated into a linear superposition of cnoidal waves plus nonlinear interactions. Can this same idea be exploited for the N-soliton solution on the infinite line? Formally, the answer is of course "yes," but as we shall see, the results are to be interpreted in a somewhat different way, i.e., as the N-soliton limit of periodic theory. To see how this occurs I now rewrite the Hirota formulation. First separate the $\underline{A}$ matrix into diagonal and off-diagonal parts $\underline{A}=\underline{D}+\underline{Q}$ and then write (3.2) in the obvious vector notation

$$F_N(\boldsymbol{\eta})=\sum_{\boldsymbol{\nu}}e^{\boldsymbol{\nu}\cdot\boldsymbol{\eta}+(1/2)\boldsymbol{\nu}^T\cdot\underline{D}\cdot\boldsymbol{\nu}}\left\{1+\frac{\sum_{\mathbf{n}}[e^{(1/2)\boldsymbol{\nu}^T\cdot\underline{Q}\cdot\boldsymbol{\nu}}-1]e^{\boldsymbol{\nu}\cdot\boldsymbol{\eta}+(1/2)\boldsymbol{\nu}^T\cdot\underline{D}\cdot\boldsymbol{\nu}}}{\sum_{\boldsymbol{\nu}}e^{\boldsymbol{\nu}\cdot\boldsymbol{\eta}+(1/2)\boldsymbol{\nu}^T\cdot\underline{D}\cdot\boldsymbol{\nu}}}\right\}\ , \tag{3.5}$$

where the integers ν_j range over (0,1). It then follows that

$$u(x,t)=2\frac{\partial^2}{\partial x^2}\ln\sum_{\boldsymbol{\nu}}e^{\boldsymbol{\nu}\cdot\boldsymbol{\eta}+(1/2)\boldsymbol{\nu}^T\cdot\underline{D}\cdot\boldsymbol{\nu}}+u_{\text{int}}(\boldsymbol{\eta})\ , \tag{3.6}$$

where

$$u_{\text{int}}(x,t)=2\frac{\partial^2}{\partial x^2}\ln\left\{1+\frac{\sum_{\nu}[e^{(1/2)\nu^T\cdot\underline{Q}\cdot\nu}-1]e^{\nu\cdot\eta+(1/2)\nu^T\cdot\underline{D}\cdot\nu}}{\sum_{\nu}e^{\nu\cdot\eta+(1/2)\nu^T\cdot\underline{D}\cdot\nu}}\right\}. \tag{3.7}$$

In analogy with Theorem 1, Eqs. (3.6) and (3.7) may be interpreted as a linear superposition of solitons plus nonlinear interactions.

To illustrate this idea I implement (3.6) and (3.7) numerically and show in Fig. 1 a two-soliton solution for which the role of phase shifting is easily observable. Then in Fig. 2 I show the linear superposition of the two solitons, i.e., the effects of nonlinear interactions u_{int} in (3.7) have been excluded. Finally, in Fig. 3 the nonlinear interactions u_{int} are shown separately. Note that the nonlinear interaction term consists simply of a negative contribution that removes each soliton from its incorrect position and then adds it back in after it has been phase shifted. Thus the idea of linearly superposed solitons plus an interaction term simply provides an alternative perspective to classical phase shifting for the physical picture of soliton collisions. The two points of view are entirely equivalent. It is clear that the interactions u_{int} can never be viewed as small with respect to the linear superposition of the solitons. Nevertheless, as discussed in more detail below, Theorem 1 remains valid and useful even when the interactions are large.

This perspective suggests, in the interest of physical

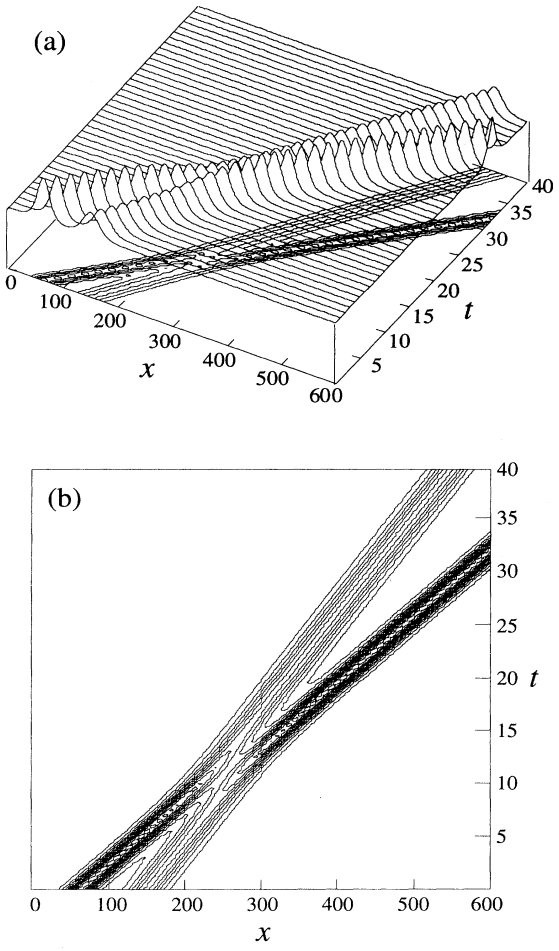

FIG. 1. Hirota two-soliton solution of the KdV equation as computed by Eqs. (3.6) and (3.7). (a) Space-time evolution. (b) Contours of the space-time evolution. The phase shifts of the solitons, due to the collision process, are clearly evident.

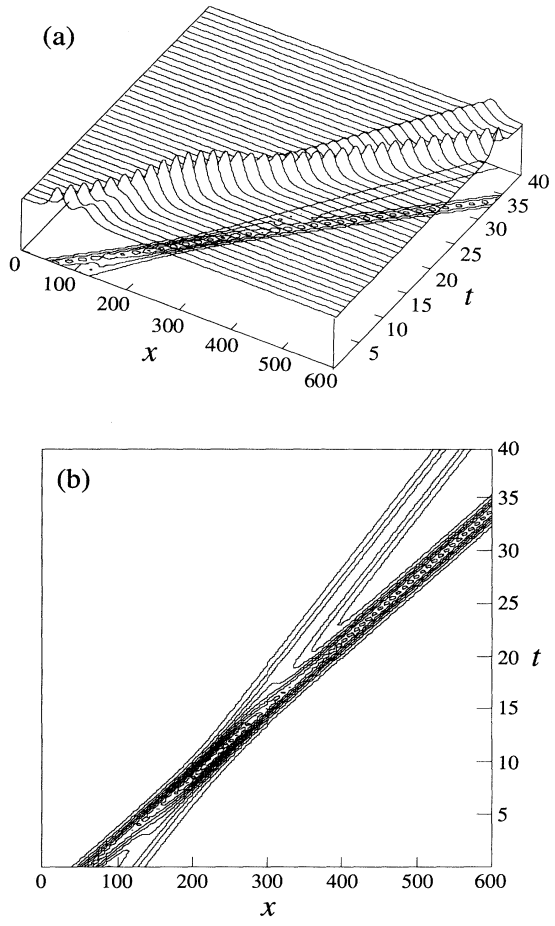

FIG. 2. Linear superposition of the two-soliton solution of Fig. 1. (a) Space-time evolution. (b) Contours of the space-time evolution. Since nonlinear interactions have been excluded, there is no phase shifting of the solitons during their collision. This example has been computed using Eqs. (3.6) and (3.7), where the nonlinear interaction term u_{int} has been set to zero.

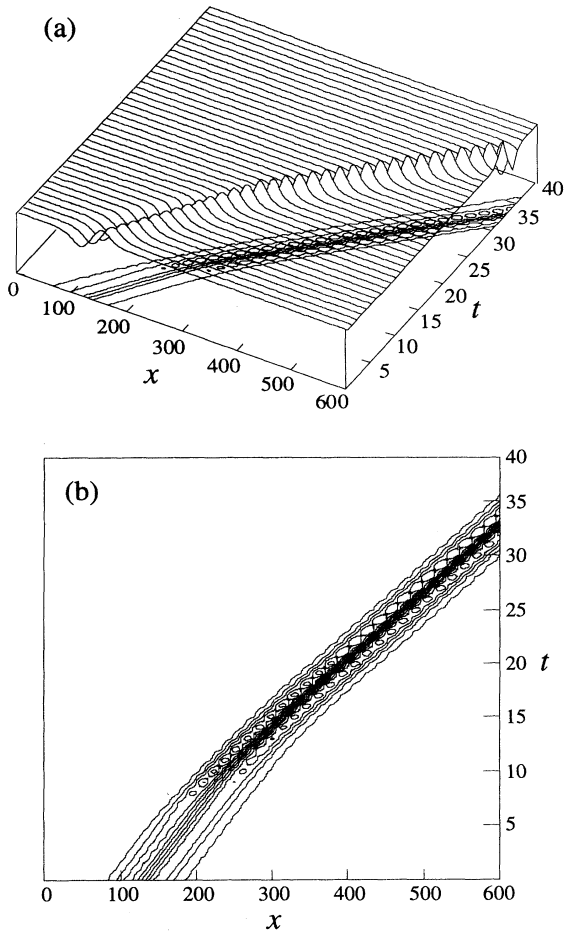

FIG. 3. Interaction contribution of the two-soliton solution of Fig. 1. This example has been computed using Eq. (3.7) to determine the nonlinear interaction term u_{int} as a function of space and time. The interaction term u_{int} shown in this figure plus the superposition of the two solitons given in Fig. 2 construct the two-soliton solution of the KdV equation shown in Fig. 1.

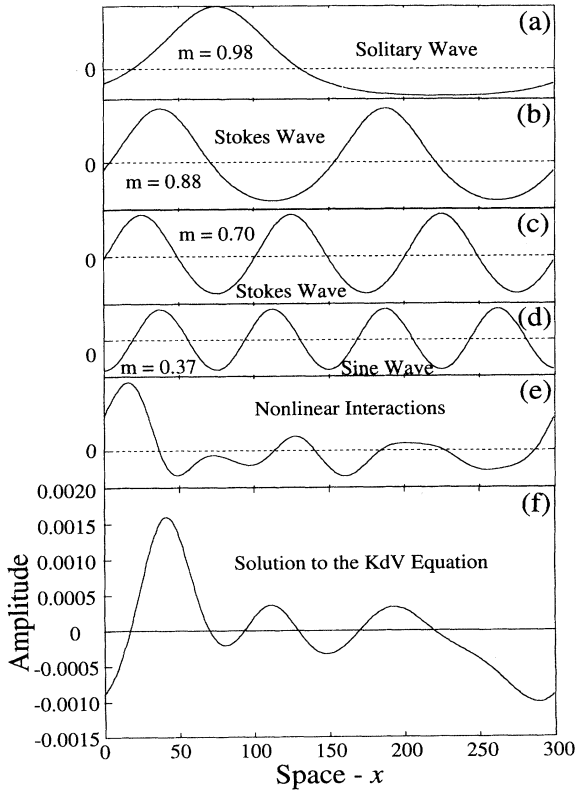

FIG. 4. Four-degree-of-freedom solution to the KdV equation. In (a)–(d) are the four cnoidal waves in the inverse scattering transform spectrum. The modulus of each component is shown in its respective panel. In (e) is the contribution due to nonlinear interactions. The four-degree-of-freedom solution to the KdV equation is given in (f) and corresponds to the linear superposition of the four cnoidal waves (a)–(d) plus nonlinear interactions (e), i.e., the sum of the curves (a)–(e).

clarity, that one might also first zero the phase shifts before the two-soliton collision, as is normally done in the literature (see [1] and references cited therein). Then after the collision one observes the resultant theoretically predicted relative phase shifts of the two solitons. However, I have not done this in the present example. Instead the numerical solution as computed by (3.1) and (3.2) is given without modification. Surprisingly, the nonlinear interaction term u_{int} takes on a life of its own, as shown in Fig. 3, and becomes a separate entity in its own right. Indeed the contribution u_{int} might loosely be referred to as "gluons" [see Figs. 3(a) and 3(b)], which serve as "intermediary particles" participating in the interaction process both before and after the collision of the solitons. This latter interpretation, together with the associated physical perspective, are of course common in elementary particle physics.

In the periodic problem the situation is perhaps even more intriguing than that just described for the infinite line. This is shown in Fig. 4 where an example is given of four cnoidal waves plus mutual nonlinear interactions. This figure emphasizes the results of Theorem 1. In the periodic problem we do not find a localized nonlinear interaction term as found in the infinite-line problem (Fig. 3). In fact, one finds a field of nonlinear interactions, distributed over the entire periodic domain. This can be seen in Figs. 5–7, where the space-time evolution of the four-degree-of-freedom system is shown. Figure 5 presents the complete nonlinear evolution of the four-cnoidal-wave solution to the KdV equation as given by formulas (2.11) and (2.12). Figure 6 instead shows the space-time evolution of the linear superposition of the cnoidal waves as computed by (2.18). Finally, in Fig. 7 the evolution of the nonlinear interaction term (2.12) u_{int} is given in the absence of other physical effects. The linear superposition of the cnoidal waves (Fig. 6) plus the interactions (Fig. 7) gives the solution to the KdV equation shown in Fig. 5. The periodic solution to the KdV equation may be thought of as a kind of ergodic "soup" in which the individual "particle" components (cnoidal waves) are continually mixing with one another as they

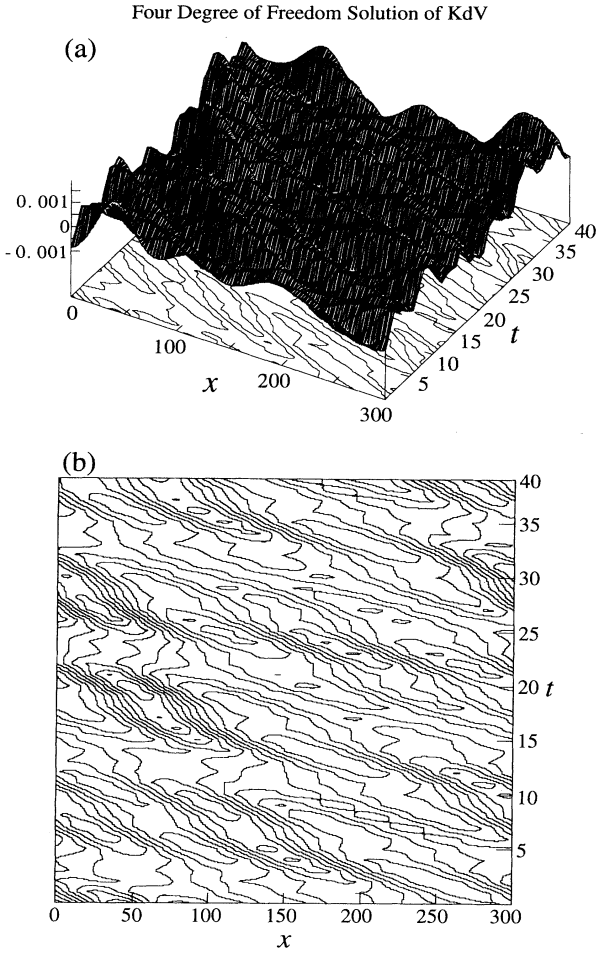

FIG. 5. Space-time evolution of the four-degree-of-freedom solution to the KdV equation shown in Fig. 4. The wave amplitudes are shown in (a), the associated contours in (b). This example has been computed using Eqs. (2.11) and (2.12).

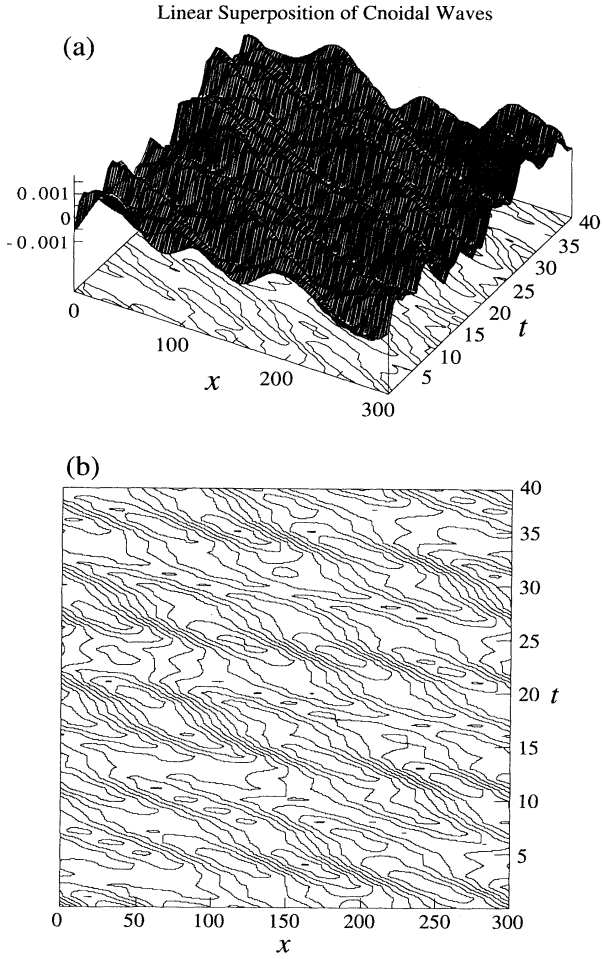

FIG. 6. Space-time evolution of the *linear superposition* of the four cnoidal waves shown in Figs. 4(a)–4(d). This example has been computed using Eq. (2.11), where the interaction term u_{int} has been set to zero. The wave amplitudes are shown in (a) and the contours in (b).

evolve and nonlinearly interact through "intermediaries" within the periodic box. All component interactions are pairwise, of course, but the infinite-line, "time-asymptotic state" in which rank-ordered solitons appear as $t \rightarrow \infty$ can never occur. Thus it is easy to physically view the present problem as a linear superposition of cnoidal waves propagating and interacting with each other in a sea of nonlinear intermediaries. By eye of course the nonlinear interaction terms are not necessarily identifiable with any single soliton-soliton (or cnoidal wave–cnoidal wave) interaction (since the effect of phase shifting may carry nonlinear interaction corrections far from the linearly superposed waves). Note that in the present case the interaction terms have a rms amplitude of about one-third of the rms amplitude of the linear superposition of the cnoidal waves (compare Figs. 6 and 7). Since the cnoidal waves generally range over a continuum of behavior for which their moduli can take on values between 0 and 1, one finds that solitons, Stokes waves, sine waves, etc., all may occur in the inverse scattering transform (IST) spectrum. This suggests that the usual clear distinction between the solitons and the radiation solutions of the infinite-line problem may be blurred in the periodic problem. The richness of the solutions of the periodic problem is further characterized by the explicit and separate representation for the nonlinear interactions as given by (2.12).

In even more complex solutions, where hundreds or even thousands of degrees of freedom occur (e.g., in stochastic processes, statistical mechanics, or ocean waves), the idea of a "background" of interactions is even more appealing, as will be seen in Sec. V. The perspective just discussed constitutes a first step toward a statistical mechanical formulation of the KdV equation [22,27].

Another important issue with regard to the concept of soliton phase shifting relates to the time series analysis of nonlinear wave trains, an example of which is also discussed in Sec. V. Given the space-time evolution of a chosen wave train, one can follow the solitons by simply

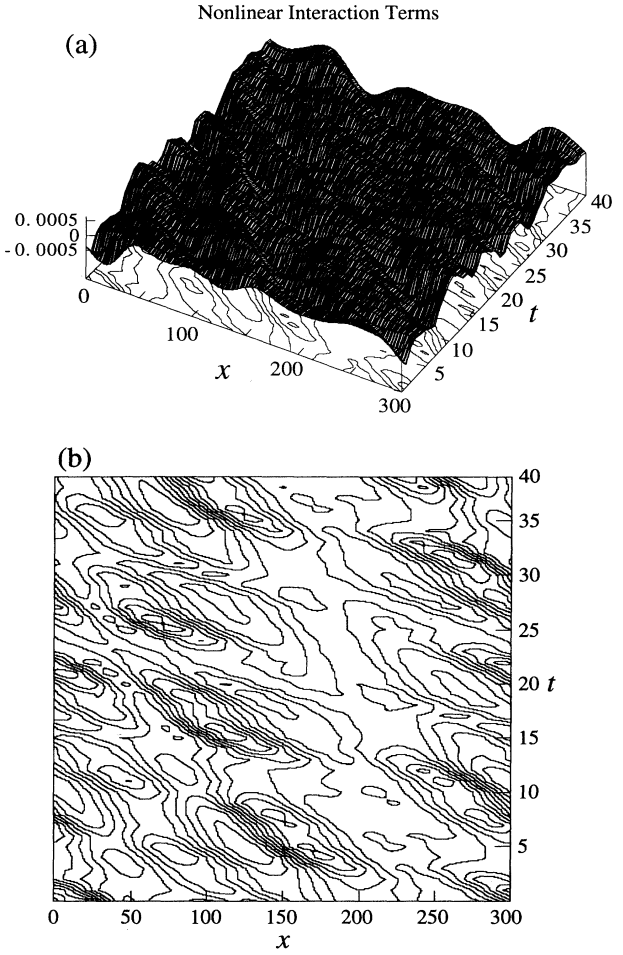

FIG. 7. Space-time evolution of the *nonlinear interactions* shown in Fig. 4(e). Here the wave amplitude consists only of the nonlinear interaction contribution u_{int} as computed using Eq. (2.12). The wave amplitudes are shown in (a) and the contours in (b).

assuming that, at a particular time $t=t_0$, the phases are identically zero, i.e., the solitons that are observable in the measured wave train are exactly where they are seen, not where they might be phase shifted relative to $t=-\infty$ or ∞. The details of this simplifying procedure, which we refer to as "phase renormalization," are deferred to a later paper on time series analysis.

IV. LINEAR FOURIER AND STOCHASTIC REPRESENTATIONS FOR THE KDV EQUATION

The Θ-function representation can, surprisingly, be written in terms of a linear Fourier series. This idea is addressed in the following theorem.

Theorem 2: Fourier theorem. The Θ function (2.2) [see also (2.7)] can be written in the form

$$\Theta_N(x,t)=\sum_{l=1}^{\infty} C_l e^{i(K_l x-\Omega_l t+\Phi_l)} ,$$
$$C_l=e^{(1/2)\mathbf{M}_l^T\cdot\underline{B}\cdot\mathbf{M}_l} , \tag{4.1a}$$

where l is an ordering parameter associated with each vector $\mathbf{M}\equiv\mathbf{M}_l$ in the Θ sum. Furthermore

$$K_l=\mathbf{M}_l\cdot\mathbf{k} , \quad \Omega_l=\mathbf{M}_l\cdot\boldsymbol{\omega} , \quad \Phi_l=\mathbf{M}_l\cdot\boldsymbol{\phi} . \tag{4.1b}$$

In these variables the inverse scattering transform in the Θ-function formulation given by (4.1) resembles linear Fourier analysis.

Proof. The Θ function (2.7) in vector form is easily written

$$\Theta_N(x,t)=\sum_{\mathbf{M}} C_{\mathbf{M}} e^{i\mathbf{M}\cdot\eta} , \quad C_{\mathbf{M}}=e^{(1/2)\mathbf{M}^T\cdot\underline{B}\cdot\mathbf{M}} . \tag{4.2}$$

By associating the integer l with each vector $\mathbf{M}$ and using (2.6) one arrives at Theorem 2. The resemblance of (4.1) to ordinary, linear Fourier analysis is, however, somewhat superficial because the commensurable wave numbers, K_l are not rank ordered with the integers as in linear Fourier analysis. Furthermore, the convergence properties of the series (4.1a) are quite different from those for linear Fourier analysis. The practical implementation of (4.1a) requires the numerical determination of large numbers of terms, even hundreds of orders of magnitude larger than for ordinary Fourier series. These ideas will be addressed in detail below in Theorem 3 and related discussions.

A. Power spectral analysis

Power spectral analysis arises from the boundary value problem for the "time KdV" (TKdV) equation [24] and its associated boundary solution $\Theta_N(0,t)$,

$$\Theta_N(x=0,t)=\sum_l C_l e^{i(\Omega_l t-\Phi_l)} . \tag{4.3}$$

This expression has the form of a linear Fourier time series. Each term in the series corresponds to a particular selection of the vector $\mathbf{M}_l$, each of which generates particular values of the scalar quantities C_l (the IST Fourier coefficients), Ω_l (the frequencies), and Φ_l (the phases). Should the phases Φ_l be uniformly distributed random numbers on the interval $(0,2,\pi)$, then the coefficients would be expressed by (see [42] and references cited therein)

$$C_l=\sqrt{2P_\Theta(\Omega_l)\Delta\Omega} , \tag{4.4a}$$

where the power spectrum of the Θ function has the form

$$P_\Theta(\Omega_l)=e^{(1/4)\mathbf{M}^T\cdot\underline{B}\cdot\mathbf{M}} . \tag{4.4b}$$

Evaluation of (4.4) must be made at the appropriate set of frequencies Ω_l, as discussed in detail below. An important ingredient missing in the formulation (4.4) is that the phases Φ_l are generally not random numbers for the KdV equation, i.e., phase locking is the natural way to construct nonlinear wave forms such as solitons and Stokes waves in the inverse scattering transform (2.1) and (2.2). This leads to technical difficulties in the derivation of the power spectrum of the solutions to the TKdV equation

$$u(0,t)=\frac{2}{c_0^2\lambda}\frac{d^2}{dt^2}\ln\Theta_N(0,t) \tag{4.5}$$

and results in necessary modifications to (4.4). These details are beyond the scope of the present paper and are therefore discussed elsewhere [36]. Nevertheless, on the basis of (4.3), together with (4.5), and assuming random phases for the cnoidal waves, it is not hard to show that a large class of solutions of the TKdV equation are stationary and ergodic.

B. Statistical properties of the wave numbers

While the form of the Fourier series given above (4.1) and (4.3) suggests that all subsequent considerations are simple, this turns out not to be the case due to mathematical difficulties, some of which I now discuss in some detail. This problem provides insight into the practical computation of Θ functions [36]. In the ordinary linear Fourier series of a periodic function the wave numbers are commensurable, i.e., recall that $\mathbf{k}=[k_1,k_2,\ldots,k_N]$, where one has the well-known result

$$k_n=n\Delta k=\frac{2\pi n}{L}\ , \quad 1\le n\le N$$

for L the spatial period of a wave train; $\Delta k=2\pi/L$ is the lowest wave number in the spectrum, which has N degrees of freedom.

How then do the wave numbers for the periodic KdV equation K_l behave for the class of Θ functions given by (4.1)? Clearly their formulation is different from those for the linear Fourier transform, i.e.,

$$K_l=\mathbf{M}_l\cdot\mathbf{k}=[M_1^l,M_2^l,\ldots,M_N^l]\cdot[1,2,\ldots,N]\Delta k$$
$$=\Delta k\sum_{n=1}^{N} nM_n^l\ . \tag{4.6}$$

This result then leads to the following theorem.

Theorem 3: Fractal index theorem. The Θ-function wave numbers K_l for the KdV equation are integer multiples I_l of Δk,

$$K_l=I_l\Delta k\ , \quad I_l=\sum_{n=1}^{N} nM_n^l \tag{4.7}$$

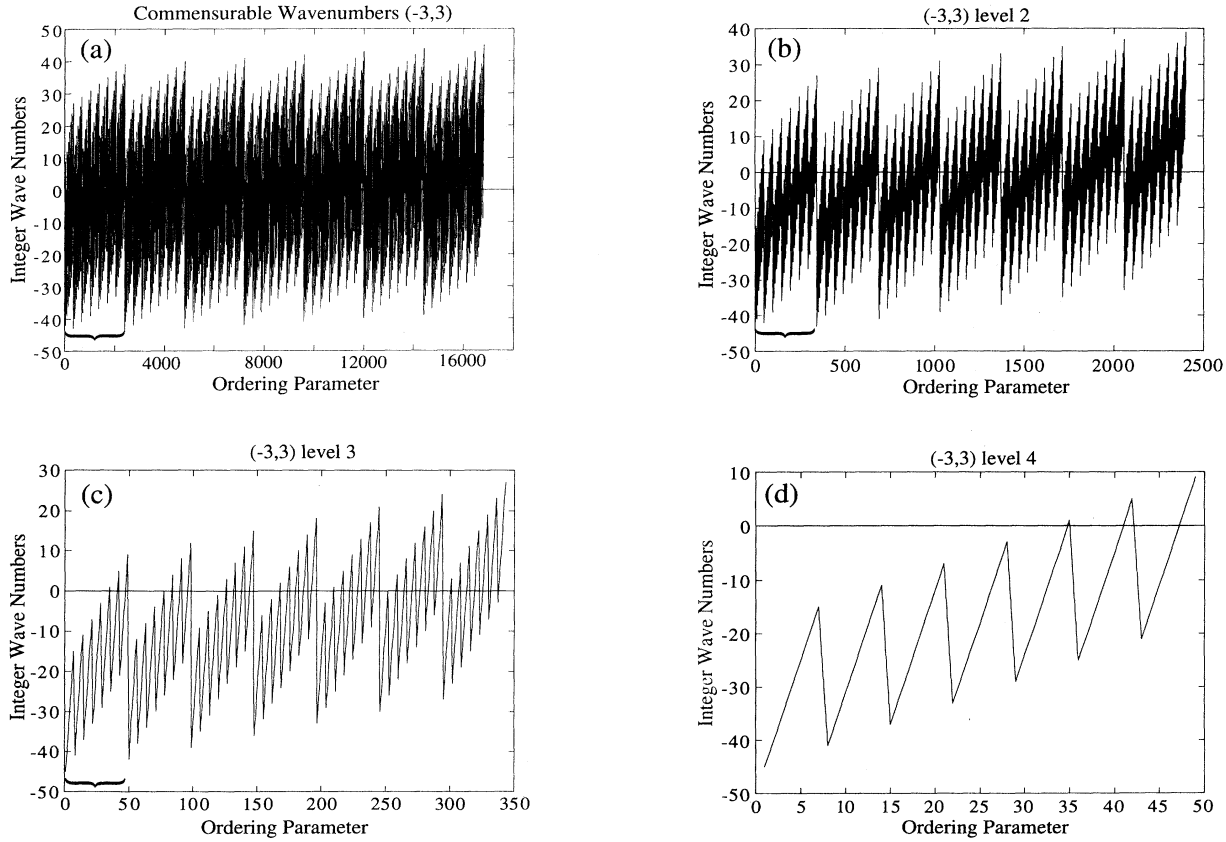

FIG. 8. Fractal commensurable wave numbers for $N=5$ degrees of freedom. The wave numbers have been computed for $M=3$ ($-3\le M_n\le 3$); there are four fractal cascades of seven levels [$(2M+1)=7$] each. The curve is space filling and has fractal dimension $D\to 2$ as $M,N\to\infty$. (b) is an exploded view of the region bracketed in (a). Note that (a) and (b) resemble each other geometrically, a result of the self-similar fractal cascading of the function. In (c) the bracketed region of (b) is exploded. The limit of the fractal scaling becomes easier to see as smaller scales are reached. Finally, the bracketed region in (c) is expanded and shown in (d). Here the scaling limit is clear and depends on the smallest wave number increment Δk.

and are therefore commensurable, possibly duplicated, and not ordered with the integers. Partial Θ sums over the individual indices M_n may be taken over arbitrary limits $(-M,M)$ rather than $(-\infty,\infty)$. Then the number of terms in the theta sum (2.2) is $(2M+1)^N+N+2$ and the number of wave numbers in the spectrum is given by $N_{\max}=[(2M+1)^N+1]$. The integer I_l is bounded, $-(J-1)\le I_l\le J$, where

$$J=M\sum_{n=1}^{N} n=\tfrac{1}{2}MN(N+1)\ . \tag{4.8}$$

$N_{\max}$ also gives the number of terms summed in the interaction contribution u_{int} in the series (2.12). It then follows that the integer function I_l is a space filling fractal function of dimension 2 as $M,N\to\infty$ [36].

Discussion of Theorem 3. Figures 8 and 9 present graphs of I_l as given by Eq. (4.7). Figure 8(a) is an example of a graph of the integer commensurable wave numbers $I_l=K_l/\Delta k$ as a function of the ordering parameter l, $1\le l\le N_{\max}$. For this particular case the summation in the Θ function is made over $-3\le M\le 3$ for a system with $N=5$ degrees of freedom, so that there are $N_{\max}=(2M+1)^N+1=7^5+1=16\,808$ wave numbers in the Θ function; $J=MN(N+1)/2=45$ so that the commensurable wave number range has the interval $-44\le I_l\le 45$. The fractal nature of the curve K_l vs l is suggested by the sequence of panels in Fig. 8. In panels (a)–(d) of the figure one can see the self-similar fractal behavior at successively smaller scales. Note that the fractal scaling (which is after all only approximate due to the finite values of M,N used in the present example) can continue downward only to the smallest possible wave number Δk.

Figure 9 gives an additional example of fractal scaling for which $N=5$ and $-5\le M\le 5$. Here too the fractal structure, down to the scale of a single wave number increment Δk, can be seen. These examples illustrate how the number of fractal cascades depends upon the parameter $2M+1$ [count seven in Fig. 8(a) and 11 in Fig. 9(a)]. The depth of the cascade depends upon the number of degrees of freedom $N-1$. In the present cases $N-1=4$; therefore, in large-degree-of-freedom systems the number of cascades is proportional to N. Hence the integer func-

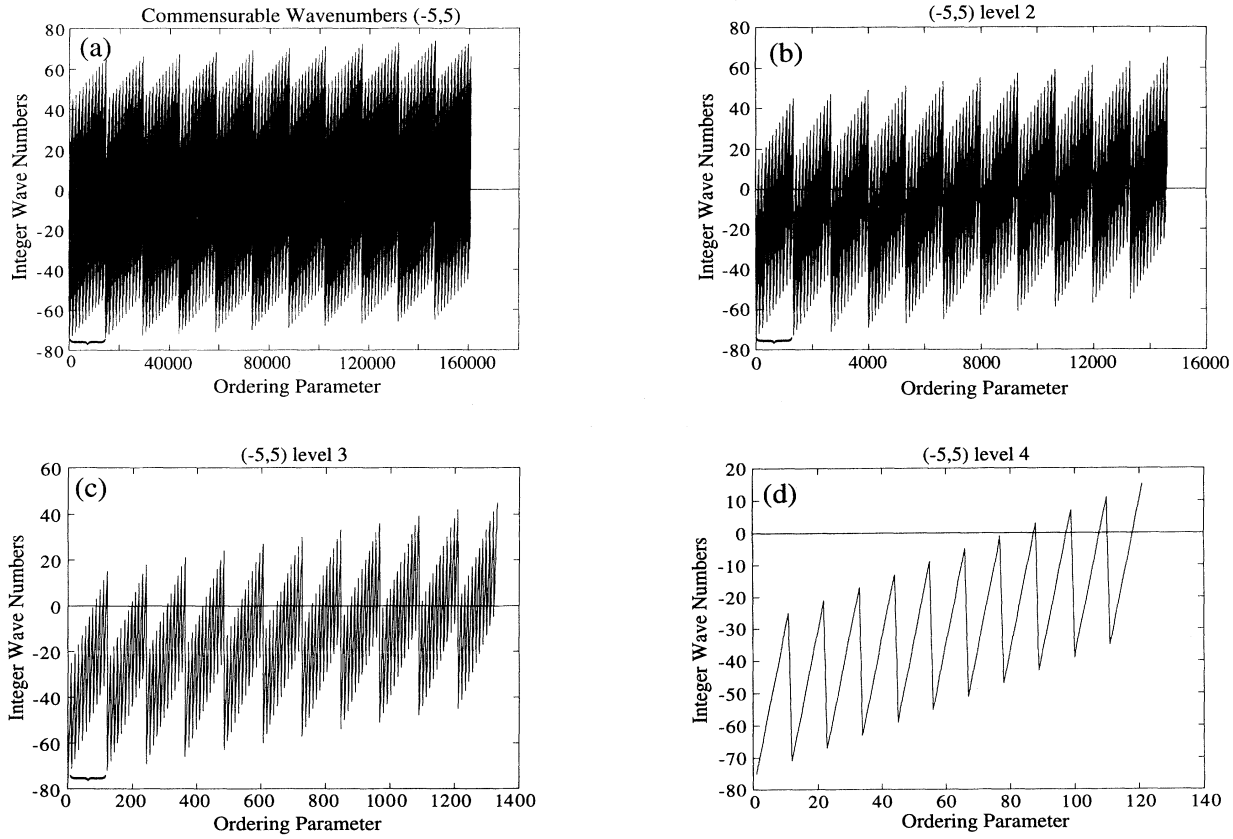

FIG. 9. Fractal commensurable wave numbers for $N=5$ degrees of freedom for $M=5$ ($-5\le M_n\le 5$); there are four fractal cascades of eleven levels $[(2M+1)=11]$ each. The curve is space filling and has fractal dimension $D\to 2$ as $M,N\to\infty$. (b) is an exploded view of the region bracketed in (a). Here (a) and (b) resemble each other geometrically, a result of the fractal cascading of the function. In (c) the bracketed region of (b) is exploded. Finally, the bracketed region in (c) is expanded and shown in (d). Here, again, the scaling limit is clear and depends on the smallest computed wave number increment Δk.

tion I_l can span several decades when N consists of several thousands of degrees of freedom. Of course, as $M,N \to \infty$ the function I_l cascades as infinite number of times over an infinite number of levels.

These surprising results should be contrasted with the usual case for the linear Fourier spectrum that has wave numbers on the interval $-5 \le I_l \le 5$, such that there are only 11 Fourier components. Clearly the periodic inverse scattering transform, which for the example of Fig. 9 has $(2M+1)^N+1=11^5+1=161\,052$ terms, is much more rich and complex than its linear Fourier counterpart.

It is not hard to see how the fractal dimension $D=2$ (Theorem 3) arises in the present problem. Simply by systematically letting M increase from $M=3$ to 5 one can see the space filling nature of the function I_l, as illustrated in the above numerical examples [e.g., Fig. 9(a) fills a blackened region of space larger than Fig. 8(a)]. Standard yardstick or scaling tests verify this conjecture; analytical and multifractal results are reported elsewhere [36].

Are there any physical manifestations of fractality in nonlinear wave motion? Evidently so, because in a recent paper by Huang *et al.* [43] the phases of the Hilbert transform of oceanic field data were found to be fractal. More recently Onorato and Osborne [44] found the wavelet transform phases of Adriatic Sea surface waves to be fractal. In light of the results developed here, further exploration of the fascinating problem of fractal properties of wave trains from the point of view of the inverse scattering transform is warranted.

Are there any additional consequences of fractality in the Θ-function representation for the present problem? The fractal properties of the integer function I_l have a substantial impact on the numerical computation of Θ-function solutions of the KdV equation via (2.1) and (2.2). This is because the number of complex exponentials that must be computed in the Θ function (2.2) is $\sim(2M+1)^N$, typically an enormous number. For example, for $M=10$, $N=1000$ (corresponding to a 2000-point time series) the number is $\sim 10^{1320}$. Modern workstations run at about 10^7 floating point operations per second. The approximate number of terms computable in the lifetime of the universe is therefore $\sim 10^{24}$, so that $\sim 10^{1296}$ universal lifetimes are required for the complete Θ-function calculating. Even if M is only 1, for $N=1000$, we get $\sim 10^{477}$ operations or 10^{453} universal lifetimes. These estimates alone suggest rather emphatically that Θ functions are not very useful for physical applications. It is fair to say that the enormous amounts of computer time required, based upon these simple estimates, have discouraged large N applications of Θ functions in soliton systems for over 20 years.

The situation is not completely hopeless, however, because the practical calculation of the Θ functions has recently been substantially improved using a fast Fourier algorithm, whose details are documented elsewhere [36] [fast inverse scattering transform (FIST)]. A major goal of this paper is to discuss present and future applications of this numerical approach to problems in nonlinear wave physics. I now address examples that illustrate why Θ functions are useful physical tools.

V. Θ-FUNCTION SOLUTIONS TO THE KdV EQUATION: EXAMPLES FROM THEORETICAL AND EXPERIMENTAL PHYSICS

How can Θ functions be useful for doing problems in wave physics? The first and most obvious way is as a tool for computing the space-time evolution of complicated solutions of the KdV equation. These include fully stochastic solutions in the sense discussed by Osborne [22]. An example is given below. Another application is as a numerical tool for the time series analysis of measured wave data. Signal processing of this type includes nonlinear filtering, an example of which is also given below. A third use is the study of coherent structures in the KdV equation. Recently Osborne and Petti [23,24] discovered experimentally that coherent structures of the KdV equation can be interpreted, for the data set investigated by them, in terms of interacting cnoidal waves with moduli in the range $\sim 0.7-0.9$. These ideas can be studied naturally in the Θ formalism as discussed herein. One should think of the Θ-function approach as extending and complimenting the work already done by the present author and co-workers on the hyperelliptic-function representation [22–27,29–35]. A number of examples are now given for application of Θ functions to problems in nonlinear wave propagation.

A. Four-degree-of-freedom solution to the KdV equation

Further discussion of Theorem 1 is in order. Illustrated in Fig. 4 is a simple four-degree-of-freedom solution to the KdV equation. Figures 4(a)–4(d) give the spectral component waves; these consist of cnoidal waves with moduli $M=0.98$, 0.88, 0.70, and 0.37. Thus one has waves corresponding roughly to a soliton, two Stokes waves, and a sine wave, respectively. The nonlinear interaction term is shown in Fig. 4(e). The linear summation of the four cnoidal waves plus nonlinear interactions is given in Fig. 4(f); this is a numerically constructed solution to the KdV equation, accurate to about 12 decimal places (for particular numerical details see Ref. [36]). A discussion of the detailed relationship of the numerical Θ-function solution to its associated hyperelliptic-function representation is also given in [36].

B. Stochastic solutions to the KdV equation

The numerical computation of the space-time evolution of solutions of the periodic KdV equation has recently been addressed by Osborne [34] in the hyperelliptic-function representation. To set the stage for numerical computation of stochastic motions it is only necessary to note that a prototypical linear stochastic process is given by the ordinary Fourier series (1.6) provided the coefficients are given by the formula

$$C_n=\sqrt{2P(f_n)\Delta f}\ ,$$

where $P(f_n)$ is the power spectrum and the phases ϕ_n are assumed to be uniformly distributed random numbers on $(0,2\pi)$.

Can a nonlinear stochastic process be defined based upon inverse scattering theory? The answer is in the affirmative; previous results have focused on the hyperelliptic-function representation [22]. In the latter nonlinear problem the IST open-band widths are the constants of the motion (these are related to the amplitudes of the cnoidal waves through algebraic geometric loop integrals; see the Appendix) and, in analogy with the linear problem, the hyperelliptic phases are chosen as uniformly distributed random numbers on the interval $(0,2\pi)$. Solutions to the periodic KdV equation of this type are fully consistent with classical stochastic representations using the linear Fourier transform (see [42] and references cited therein). In the present paper I extend the notion of nonlinear stochastic solutions of the KdV equations by implementing the Θ-function representation. Here the cnoidal wave phases are taken to be uniformly distributed random numbers on $(0,2\pi)$.

To this end the space-time evolution of a stochastic 128-degree-of-freedom solution to the KdV equation is given in Fig. 10. As with Osborne [22] the spectrum has been chosen to be a power law $\sim f^{-\alpha}$, $\alpha=2.0$. The spectrum contains 9 solitons ($m>0.99$) and 119 radiation

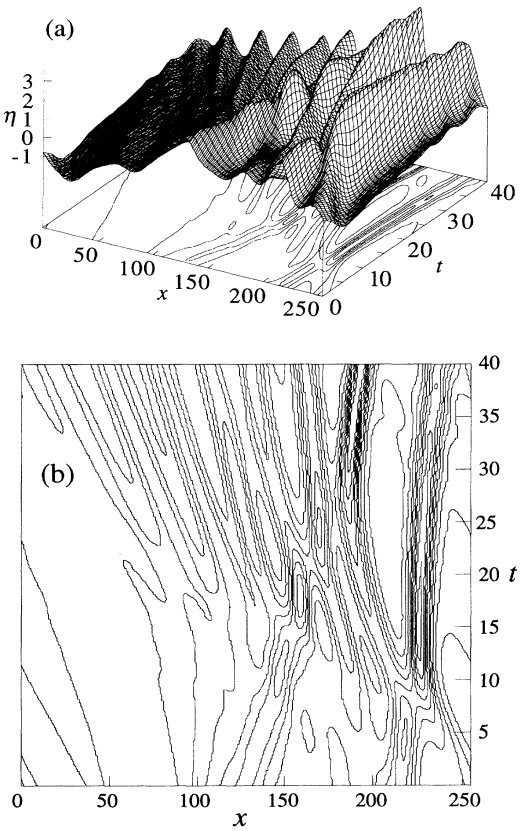

FIG. 10. (a) Space-time diagram of a 128-degree-of-freedom stochastic solution (power spectrum $\sim f^{-\alpha}$, $\alpha=2.0$) to the KdV equation as computed in the Θ-function representation. The Θ phases Φ_l have been selected to be uniformly distributed random numbers on the interval $(0,2\pi)$. The spectrum has 9 solitons and 119 radiation components. (b) Contour plot of the space-time evolution.

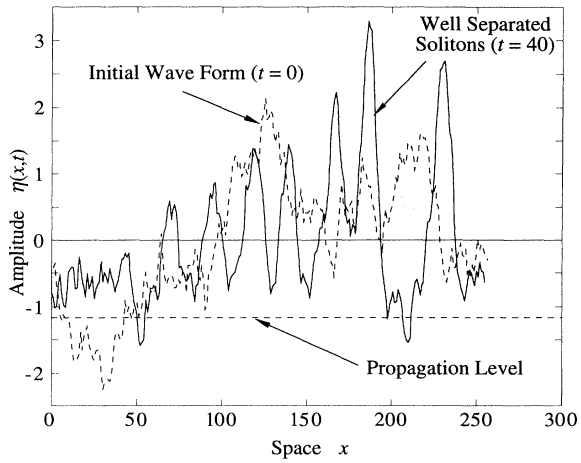

FIG. 11. Stochastic solution to the KdV equation from Fig. 10 at $t=0$ and 40. No solitons are visible in the initial conditions (dotted line), while at the later time the solitons are easily visible (solid line). This result illustrates how purely stochastic solutions to the KdV equation can have space-time dynamics consisting of solitons in a random sea of radiation. These results are computed by the FIST algorithm in Ref. [36].

modes ($m<0.5$). The cnoidal wave phases have been chosen to be uniformly distributed random numbers on the interval $(0,2\pi)$. The FIST algorithm [36] has been used to perform the calculation; the associated finite-gap spectrum is also discussed in [36]. In Fig. 10 I graph this solution of the KdV equation at the time $t=0$ and then evolve it forward in time using the fast Θ-function formulation. The evolution has been halted at a moment when the solitons in the spectrum are widely separated in physical space ($t=40$, Fig. 11), exactly at the same point computed by Osborne in the hyperelliptic-function representation [22]. It is clear that stochastic solutions of this type may be interpreted in terms of randomly interacting solitons in a random sea of radiation. In the present application the Θ-function representation is much faster for numerical computations than its close cousin, the hyperelliptic-function representation; furthermore, Θ functions do not exhibit the numerical pathologies that occur in the computation of the hyperelliptic functions [34]. It should be clear that fast computation of Θ-function solutions of this type opens the way to fast nonlinear power spectral analysis for computational and time series analysis applications. An important property of the space-time simulations of this 128-degree-of-freedom solution is the stationarity and the ergodicity of the solutions; proof of this assertion, based upon certain physical considerations, is given elsewhere [36].

C. Analysis of oceanic wave trains

Unidirectional oceanic wave trains in shallow water have recently been analyzed using the inverse scattering transform in the hyperelliptic-function representation [25,26]. Here I give an analysis of an oceanic wave train using the Θ-function representation. The measured wave

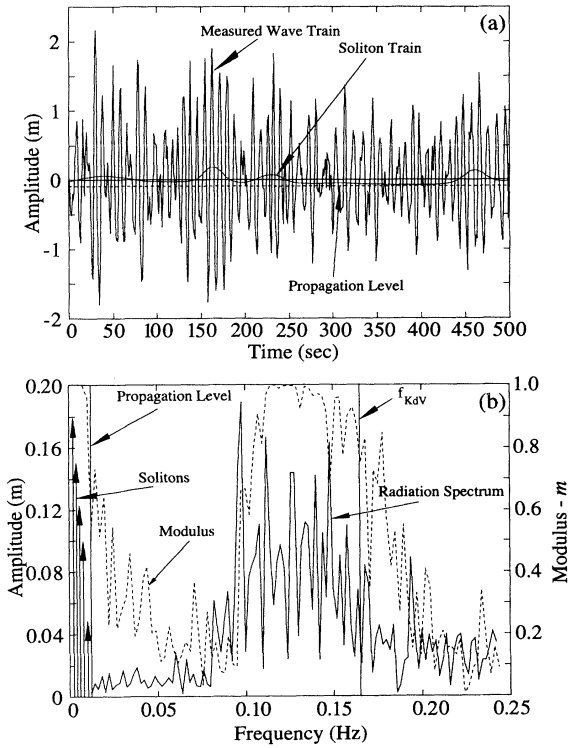

FIG. 12. Θ-function inverse scattering transform analysis of surface wave data measured in the Adriatic Sea. The measured wave train is shown in (a). In (b) is the inverse scattering transform of the data given in (a); the solid jagged curve represents the oscillatory modes in the spectral peak and the vertical arrows denote the "infinite-line" solitons. Each spectral amplitude corresponds to the amplitude of its associated cnoidal wave. The values of the spectral modulus m for each cnoidal wave component are also shown. Values of $m \sim 1$ indicate the presence of solitons (to the left, at low frequency) or soliton trains (to the right, at intermediate frequency).

train has been obtained in the Adriatic Sea and is shown in Fig. 12(a), while the scattering transform Θ-function spectrum is graphed in Fig. 12(b). The wave train has 2000 points and hence the number of degrees of freedom is $N=1000$; only 125 degrees of freedom have been graphed in the present example [Fig. 12(b)]; in the Θ-function representation the spectrum is synonymous with the amplitudes of the cnoidal waves graphed as a function of frequency. From the figure it is clear that the spectrum can be easily divided into well-defined solitons and a spectral peak near 0.1 Hz. Five solitons are found in the spectrum; the spectral peak, however, dominates the motion energetically. Also graphed are the moduli m of the cnoidal wave components. The fact that the moduli are near 1 at low frequency provides the soliton interpretation for the lowest five modes. The moduli then decrease for somewhat higher frequencies, but increase again to values near ~ 1 for intermediate values of the frequency (coinciding with the spectral peak). The moduli generally decrease again for still higher frequency; this latter decrease is consistent with the well-known linearization of the KdV equation dynamics at high frequency.

The fact that $m \sim 1$ at intermediate frequencies implies that the most energetic part of the spectral peak is interpretable in terms of solitons. This is a surprising fact and deserves further attention. In the spectral peak it is important to note that the frequencies are relatively high, i.e., they behave like $\omega_n = 2\pi n/T$, where n is the number of the spectral component, for T the temporal period of the measured wave train. The region near the peak for which $m \sim 1$ corresponds to $n \sim 50-70$ oscillations per period T. This suggests that the IST components in the spectral peak might well oscillate much like sine waves, i.e., they could have a form similar to the rapidly oscillating function $\sin\omega_n t$. Of course, the components are *not* sine waves in this nonlinear case; they are cnoidal waves, each with its own modulus m. Consequently, each component in the spectral peak for which $m \sim 1$ is a soliton train, i.e., it is shaped like a sequence of many solitons (n of them within the temporal period T), one after the other, of equal amplitude (see Ref. [15] for a discussion of this concept). Wave trains of this type are a succession of equal-amplitude sharp peaks and shallow troughs, each indistinguishable from a soliton inside a single period T/n. On the basis of the analysis of the Adriatic Sea data (Fig. 12) and Theorem 1 we therefore conclude that the most nonlinear part of the measured spectral peak (where $m \sim 1$) consists of a linear superposition of soliton trains that are nonlinearly interacting with each other.

The interpretation of the peak in terms of soliton trains or nonlinear oscillatory modes is quite recent and suggests that a detailed and separate study is in order; extensive discussion has therefore been delayed to a future paper. Note, however, that no analog exists for soliton trains in the spectrum for the infinite-line problem. However, Ablowitz and Segur [1] have pointed out, based upon an asymptotic analysis, that the first maximum in the radiation tail of the infinite-line problem (as $t \to \infty$) has a shape that is indistinguishable from a single soliton.

By addressing the spectral peak in terms of the interaction matrix $\underline{B}$ in the Θ-function formulation it is possible to filter out the peak modes and to directly observe the infinite-line solitons as shown in Fig. 12(a). This is done by first selecting the 5×5 submatrix corresponding to the soliton part of the spectrum, which resides in the upper left-hand corner of the $\underline{B}$ matrix (in the present case $\underline{B}$ has been taken to be 125×125). The soliton train in Fig. 12(a) corresponds to the numerical computation of Eqs. (2.1) and (2.2) using this 5×5 matrix. An advantage of the Θ-function formulation for nonlinear filtering is that the procedure is quite straightforward, requiring only a single operation [e.g., evaluation of (2.1) and (2.2) for a five-degree-of-freedom matrix), while for the hyperelliptic-function formulation an iterative procedure is necessary [35]. It goes without saying that this filtering approach will have a considerable number of applications in future experimental studies. Spectral decomposition of the peak of the spectrum in terms of soliton trains is discussed in detail elsewhere [36].

The results given herein suggest that a nonlinear Adriatic Sea wave train has relatively few nonlinear modes,

i.e., $N \sim 5$ for the solitons and $N \sim 10$ for the soliton trains in the spectral peak, for a total of about 15 energetically dominant modes. It is worthwhile noting that the high-frequency tail of the wave spectrum [which behaves roughly as a power law such that $P(f) \sim f^{-4} - f^{-5}$] is due mainly to wind-forcing dynamics. Thus, while local wave dynamics may be governed by a few dominant nonlinear degrees of freedom, the global wind-driven dynamics arise in the relatively small-amplitude power-law tail of the spectrum, which is neglected in the present analysis.

It is worth pointing out that the FIST algorithm has been used in two ways in the present applications: first, with regard to the time evolution discussed in Figs. 10 and 11, where the algorithm uses computer time proportional to MN^4. For the data analysis applications as shown in Fig. 12, the algorithm is proportional to MN^3. One can ask, How can such a drastic reduction be obtained in view of the results of Theorem 3? The answer is that while there is a large amount of complexity in the Θ-function formulation, much of it is repetitive, or nearly so, in the fractal scaling process and this leads to recursion relations over the fractal cascades. As discussed above, the number of cascades, and hence the number of recursion steps, is finite for finite M and N. Details of these algorithms are given in Ref. [36].

VI. CONCLUSIONS

The Θ-function representation of the inverse scattering transform for the Korteweg–deVries equation with periodic boundary conditions has been discussed. It is shown that the Θ-function formulation consists of a linear superposition of cnoidal waves plus nonlinear interactions. Furthermore, it is shown that while the wave numbers of the Θ-function formulation for the KdV equation are commensurable, they are also fractal functions of the ordering parameter l. Nonlinear power spectral analysis is a natural consequence of the method and stochastic solutions of the KdV equation may be readily computed. To this end a fast Fourier algorithm (FIST) for computing solutions to the KdV equation is exploited. Numerical computations of space-time solutions of the KdV equation, statistical mechanical interpretations of the motion, stochastic solutions, and broadband spectral analysis of time series of oceanic data are among the principal applications of the methods discussed therein.

One should think of the Θ-function approach as extending and complimenting the work previously done by the present author and co-workers on the hyperelliptic function representation [22–27,29–35]. An observation is that the Θ-function approach for describing nonlinear wave trains in terms of cnoidal waves plus interactions is particularly useful for systems with relatively many degrees of freedom. In this case the interaction terms take on the form of a background flux of intermediaries, which mediate cnoidal wave interactions in solutions of the KdV equation. This perspective for the KdV periodic problem is analogous to the phase shift interpretation of soliton interactions for the infinite-line problem. Evidently, broadband wave train solutions to the KdV equation consists of two kinds of solitons (corresponding to spectral regions in which $m \sim 1$), e.g., (i) infinite-line solitons, which appear once in the spatial period L of the wave train at low wave numbers, and (ii) soliton wave trains, which may oscillate many times within the period L at intermediate wave numbers.

An associated relevant discovery is that there exists a class of cnoidal wave solutions to the KdV equation such that each cnoidal wave occurs only once in the period L and has relatively large modulus $m > 0.7$ [23,24]; in fact, there may be more than one such single-period cnoidal wave in a given wave train. These solutions have been loosely termed "coherent structures" in [23,24]. This perspective contrasts with previous interpretations of coherent structures (in integrable wave equations) as being solitons. The results given by Osborne and Petti [23,24] thus extend the definition of coherent structures to include also signal cnoidal waves of large modulus. It is expected that the Θ-function approach addressed herein will shed light on wave trains of this type.

From the author's point of view the perspective of the present paper can be summarized as follows. For nearly two centuries the Fourier transform has been used to obtain information about a wide variety of both linear and nonlinear wavelike physical systems. Linear Fourier analysis provides the investigator with the mathematical tools for obtaining the amplitudes and phases of the particular sine waves, which when linearly superposed, give back the wave train under study. Generally speaking, the Fourier amplitudes and phases are constants of the motion in linear systems, but have varying space-time dynamics in nonlinear systems. There is no doubt that the linear Fourier approach is among the most used and well-liked methods in the field of experimental data analysis. Yet the information content of Fourier analysis often cannot directly address many of the nonlinear effects in physical systems. However, with the Θ-function representation of the periodic inverse scattering transform, one is able to directly project the motion onto the "true" modes (the cnoidal or the traveling-wave solutions) of a system governed by a particular nonlinear, integrable wave equation. One can therefore answer some of the following questions about a measured, nonlinear wave train using the Θ-function representation.

(i) Where are the solitons in the measured wave train?

(ii) Where are the oscillatory modes in the measured data?

(iii) Where are the coherent structures in the data?

(iv) What is the nonlinear spectral decomposition of the oscillatory modes in the measured wave train?

(v) Where are the soliton trains that form the most nonlinear part ($m \sim 1$) of the oscillatory modes?

(vi) How do the nonlinear components (cnoidal waves) interact with each other (both pair-wise and globally) in the measured wave train?

(vii) How does one specifically obtain the contribution due to nonlinear interactions in the measurements?

Detailed documentation of the above capabilities is given

in Ref. [36]. Here are some advantages that Θ functions have over the hyperelliptic function.

(i) With Θ functions one can directly access, investigate, and extract each soliton in the spectrum through a nonlinear filtering procedure. With the hyperelliptic functions one can access only that part of the wave train that contains all the solitons together with their requisite interactions; individual solitons can never be filtered out of the measured wave train [35].

(ii) With Θ functions one can access the pairwise nonlinear (cnoidal wave–cnoidal wave) interactions through nonlinear filtering techniques (Fig. 4). Nonlinear interactions can never be directly computed with the hyperelliptic functions in the filtering process because the interactions cannot be explicitly separated from the hyperelliptic functions themselves.

(iii) With Θ functions one can perform nonlinear filtering in a single step. Nonlinear filtering with the hyperelliptic functions is an iterative process [35].

(iv) With the Θ functions one accesses the physically relevant spectral components that are the cnoidal waves themselves (they are solutions of the KdV equation) rather than the hyperelliptic functions (which are not individually solutions of the KdV equation). The individual Θ functions can be computed in a single step. The hyperelliptic functions must be computed iteratively.

(v) Hyperelliptic functions are hard to compute numerically directly from their respective ordinary differential equations because of ill conditioning near the band edges (or branch points) in the Floquet spectrum [34]. The Θ functions are easier to compute because they are not ill conditioned anywhere in the spectrum.

All of these issues, and their implementation in terms of the Θ-function representation, address the physical understanding of fundamental nonlinear effects in measured wave trains. After applying Θ functions to a variety of nonlinear problems it has become clear that the linear Fourier transform is not a very precise picture of nonlinear wave motions. The nonlinear modes for the KdV equation are not sine waves; they are interacting cnoidal waves. In the author's opinion the implications of this perspective on experiments and data analysis will be far reaching and could well enhance our future appreciation and understanding of nonlinear effects over a broad spectrum of physical phenomena in a wide variety of physical systems.

ACKNOWLEDGMENTS

This work was supported in part by the U. S. Office of Naval Research (Grant No. N00014-92-J-1330) and by project Progetto Salvaguardia di Venezia of the Consiglio Nazionale delle Ricerche, Italy.

APPENDIX: COMPUTATION OF WAVE NUMBERS, FREQUENCIES, PHASES, AND INTERACTION MATRIX IN THE Θ-FUNCTION REPRESENTATION

This appendix summarizes the determination of the wave numbers k_j, frequencies ω_j, phases ϕ_j, and the period or interaction matrix $\underline{B}$ in the Θ-function solution to the KdV equations (2.1)–(2.3) [10–16]; see also [1]. The formulation discussed in this appendix is the N-dimensional generalization of the classical Jacobian elliptic integrals [38,39]. Although some knowledge of algebraic geometry is necessary for the derivation of the following formulas, the results can be implemented numerically with only rudimentary understanding of algebraic-geometric methods [36].

The Θ function is 2π periodic in each of the N phases η_j

$$\Theta((\eta_1+2\pi),(\eta_2+2\pi),\ldots,(\eta_N+2\pi)) = \Theta(\eta_1,\eta_2,\ldots,\eta_N) . \quad \text{(A1)}$$

Normalized holomorphic differentials on the Riemann surface Γ are then introduced

$$d\Omega_n(E)=\sum_{m=1}^{N} C_{nm}\frac{E^{m-1}dE}{R^{1/2}(E)} , \quad \text{(A2)}$$

where $R(E)$ is given by

$$R(E)=\prod_{k=1}^{2N+1}(E-E_k)$$

and the following normalization condition is assumed to hold:

$$\oint_{\alpha_j} d\Omega_n(E)=2\pi i\delta_{nj} . \quad \text{(A3)}$$

These are the "α_j cycles" or contour integrals around the open band (E_{2j},E_{2j+1}) in the Floquet spectrum. Combining (A2) and (A3) provides the relations

$$\sum_{m=1}^{N} C_{nm}J_{mj}=2\pi i\delta_{nj} , \quad J_{mj}=\oint_{\alpha_j}\frac{E^{m-1}dE}{R^{1/2}(E)} , \quad \text{(A4)}$$

which in matrix notation give

$$\underline{C}=2\pi i\underline{J}^{-1} . \quad \text{(A5)}$$

The normalization coefficients C_{nm} in (A2) are then given by [34]

$$C_{jm}=2\pi i\left[\oint_{\alpha_j}\frac{E^{m-1}dE}{\left[\prod_{k=1}^{2N+1}(E-E_k)\right]^{1/2}}\right]^{-1} = \pi i\left[\int_{E_{2j}}^{E_{2j+1}}\frac{E^{m-1}dE}{\left[\prod_{k=1}^{2N+1}(E-E_k)\right]^{1/2}}\right]^{-1} . \quad \text{(A6)}$$

Note that each loop integral has been reduced to an ordinary definite integral across an open band in the Floquet spectrum. The phases η_j of the Θ function (2.2) are found by the Abelian integrals

$$\eta_j(P_1,P_2,\ldots,P_j)=-i\sum_{m=1}^{N}\int_{E_{2m}}^{P_m(x,t)} d\Omega_j(E) = k_jx-\omega_jt+\phi_j , \quad \text{(A7)}$$

where ω_j is given by the second equation of (A8) below

and $P_m(x,t)=[\mu_m(x,t),\sigma_m]$ for $1\le m\le j$. Equation (A7) may be interpreted as a linearization of the hyperelliptic-function representation of the flow, i.e., integration over the holomorphic differentials (A2) from the lower band edge E_{2j} to the hyperelliptic functions $\mu_j(x,t)$ in effect linearizes the μ_j (intrinsically nonlinear functions that provide the solution to the KdV equation through a linear superposition law) whose numerical evolution is described in detail elsewhere [34]. This leads to the linear Θ-function inverse problem for the KdV equation described in Sec. II. Equations (A2) and (A7) are an Abel transform pair. Generally speaking, the phase of the hyperelliptic functions η_j (A7) depends upon the main spectrum (E_i, $1\le i\le 2N+1$) and the space-time evolution of the auxiliary spectrum $[\mu_j(x,t),\sigma_j]$, $1\le j\le N$.

It then follows that the wave numbers k_j and frequencies ω_j are given by

$$k_j=2C_{N,j}\ ,$$
$$\omega_j=8C_{N-1,j}+4C_{N,j}\sum_{i=1}^{2N+1}E_i\ . \tag{A8}$$

Both k_j and ω_j are real constants since the C_{jm} and the E_k are the real constants. The usual dispersion law for a single degree of freedom may easily be obtained [34]. The k_j are commensurable wave numbers in the cycle integral basis considered here, while the frequencies ω_j are generally incommensurable.

The phases ϕ_j are found by fixing $x=0$ and $t=0$ in (A7) to get

$$\phi_j=-i\sum_{m=1}^{N}\int_{E_{2m}}^{P_m(0,0)}d\Omega_j(E)$$
$$=-i\sum_{m=1}^{N}C_{jm}\int_{E_{2m}}^{\mu_m(0,0)}\frac{E^{m-1}dE}{R^{1/2}(E)}=-i\sum_{m=1}^{N}C_{jm}\Phi_m\ , \tag{A9}$$

where

$$\Phi_m=\int_{E_{2m}}^{\mu_m(0,0)}\frac{E^{m-1}dE}{R^{1/2}(E)}\ . \tag{A10}$$

Thus the constant phases ϕ_j of the hyperelliptic functions depend upon the starting values of the hyperelliptic functions $\mu_j(0,0)$ and the Riemann sheet indices σ_j.

The period matrix is given by

$$B_{nj}=\oint_{\beta_j}d\Omega_n(E)=\sum_{m=1}^{N}C_{nm}\oint\frac{E^{m-1}dE}{R^{1/2}(E)}=\sum_{m=1}^{N}C_{nm}B_{mj}\ , \tag{A11}$$

where

$$B_{mj}=2\int_{E_1}^{E_{2j}}\frac{E^{m-1}dE}{R^{1/2}(E)}\ , \tag{A12}$$

where the integrals are over the "β cycles" of the theory (for a discussion with regard to the numerical analysis see Ref. [36]). A fast numerical algorithm for computing Θ functions is discussed elsewhere [36].

[1] M. J. Ablowitz and H. Segur, *Solitons and the Inverse Scattering Transform* (SIAM, Philadelphia, 1981).
[2] R. K. Dodd, J. C. Eilbeck, J. D. Gibbon, and H. C. Morris, *Solitons and Nonlinear Wave Equations* (Academic, London, 1982).
[3] A. C. Newell, *Solitons in Mathematics and Physics,* (SIAM, Philadelphia, 1985).
[4] V. E. Zakharov, S. V. Manakov, S. P. Novikov, and M. P. Pitayevsky, *Theory of Solitons. The Method of the Inverse Scattering Problem* (Nauka, Moscow, 1980).
[5] M. J. Ablowitz and P. A. Clarkson, *Solitons, Nonlinear Evolution Equations and Inverse Scattering* (Cambridge University Press, Cambridge, 1991).
[6] A. Degasperis, in *Nonlinear Topics in Ocean Physics,* edited by A. R. Osborne (Elsevier, Amsterdam, 1991).
[7] M. Boiti, F. Pempinelli, and A. Pogrebkov, J. Math. Phys. (to be published); M. Boiti, L. Martina, and F. Pempinelli (unpublished).
[8] G. B. Whitham, *Linear and Nonlinear Waves* (Wiley, New York, 1974).
[9] J. W. Miles, Ann. Rev. Fluid Mech. **12**, 11 (1980).
[10] A. R. Its and V. B. Matveev, Func. Anal. Appl. **9**, 65 (1975).
[11] B. A. Dubrovin, V. B. Matveev, and S. P. Novikov, Russ. Math. Surv. **31**, 59 (1976).
[12] H. Flaschka and D. W. McLaughlin, Prog. Theor. Phys. **55**, 438 (1976).
[13] E. Date and S. Tanaka, Prog. Theor. Phys. Suppl. **59**, 107 (1976).
[14] H. P. McKean and E. Trubowitz, Commun. Pure Appl. Math. **29**, 143 (1976).
[15] W. E. Ferguson, Jr., H. Flaschka, and D. W. McLaughlin, J. Comput. Phys. **45**, 157 (1982).
[16] M. G. Forest and D. W. McLaughlin, J. Math. Phys. **23**, 1248 (1982).
[17] J. P. Boyd, J. Math. Phys. **25**, 3390 (1984).
[18] J. P. Boyd, J. Math. Phys. **25**, 3402 (1984).
[19] J. P. Boyd, J. Math. Phys. **25**, 3415 (1984).
[20] J. P. Boyd and S. E. Haupt, in *Nonlinear Topics in Ocean Physics,* edited by A. R. Osborne (Elsevier, Amsterdam, 1990).
[21] J. P. Boyd, Adv. Appl. Mech. **27**, 1 (1990).
[22] A. R. Osborne, Phys. Rev. Lett. **71**, 3115 (1993).
[23] A. R. Osborne and M. Petti, Phys. Rev. E **47**, 1035 (1993).
[24] A. R. Osborne and M. Petti, Phys. Fluids **6**, 1727 (1994).
[25] A. R. Osborne, in *Proceedings of the Aha Huliko'a Hawaiian Winter Workshop,* edited by Peter Müller and Diane Henderson (University of Hawaii Press, Honolulu, 1993).
[26] A. R. Osborne, L. Bergmasco, M. Serio, and L. Cavaleri (unpublished).
[27] A. R. Osborne (unpublished).
[28] V. I. Karpman, *Nonlinear Waves in Dispersive Media* (Pergamon, Oxford, 1975).
[29] A. R. Osborne, in *Statics and Dynamics of Nonlinear Systems,* edited by G. Benedek, H. Bilz, and R. Zeyher

(Springer-Verlag, Heidelberg, 1983).
[30] A. R. Osborne and L. Bergamasco, Nuovo Cimento B **85**, 2293 (1985).
[31] A. R. Osborne and L. Bergamasco, Physica D **18**, 26 (1986).
[32] A. R. Osborne, in *Nonlinear Topics in Ocean Physics,* edited by A. R. Osborne (North-Holland, Amsterdam, 1991).
[33] A. R. Osborne, J. Comput. Phys. **94**, 284 (1991).
[34] A. R. Osborne, Phys. Rev. E **48**, 296 (1993).
[35] A. R. Osborne, J. Math. Comput. Sim. **37**, 431 (1994).
[36] A. R. Osborne (unpublished).
[37] D. J. Korteweg and G. deVries, Philos. Mag. Ser. **5**, 422 (1895).
[38] *Handbook of Mathematical Functions,* Natl. Bur. Stand. Appl. Math. Ser. No. 55, edited by M. Abramowitz and I. A. Stegun (U. S. GPO, Washington, DC, 1964).
[39] W. Magnus, F. Oberhettinger, and R. P. Soni, *Formulas and Theorems for the Special Functions of Mathematical Physics* (Springer-Verlag, New York, 1966).
[40] R. Flesch, M. G. Forest, and A. Sinha, Physica D **48**, 169 (1991).
[41] D. W. McLaughlin and C. M. Schober, Physica D **57**, 447 (1992).
[42] A. R. Osborne, in *Topics in Ocean Physics,* edited by A. R. Osborne and P. Malanotte-Rizzoli (North-Holland, Amsterdam, 1982), p. 515.
[43] N. E. Huang, S. R. Long, C.-C. Tung, M. A. Donelan, Y. Yuan, and R. J. Lai, Geophys. Res. Lett. **19**, 685 (1992).
[44] M. Onorato and A. R. Osborne (unpublished).